Thermohaline Stratification of the Indonesian Seas: Model and Observations*

Arnold L. Gordon

Lamont-Doherty Earth Observatory of Columbia University, Palisades, New York

Julie L. McClean

Department of Oceanography, Naval Postgraduate School, Monterey, California

ABSTRACT

The Indonesian Throughflow, weaving through complex topography, drawing water from near the division of the North Pacific and South Pacific water mass fields, represents a severe challenge to modeling efforts. Thermohaline observations within the Indonesian seas in August 1993 (southeast monsoon) and February 1994 (northwest monsoon) offer an opportunity to compare observations to model output for these periods. The simulation used in these comparisons is the Los Alamos Parallel Ocean Program (POP) 1/6 deg (on average) global model, forced by ECMWF wind stresses for the period 1985 through 1995. The model temperature structure shows discrepancies from the observed profiles, such as between 200 and 1200 dbar where the model temperature is as much as 3°C warmer than the observed temperature. Within the 5°–28°C temperature interval, the model salinity is excessive, often by more than 0.2. The model density, dominated by the temperature profile, is lower than the observed density between 200 and 1200 dbar, and is denser at other depths. In the model Makassar Strait, North Pacific waters are found down to about 250 dbar, in agreement with observations. The model sill depth in the Makassar Strait of 200 m, rather than the observed 550-m sill depth, shields the model Flores Sea from Makassar Strait lower thermocline water, causing the Flores lower thermocline to be dominated by salty water from the Banda Sea. In the Maluku, Seram, and Banda Seas the model thermocline is far too salty, due to excessive amounts of South Pacific water. Observations show that the bulk of the Makassar throughflow turns eastward into the Flores and Banda Seas, before exiting the Indonesian seas near Timor. In the model, South Pacific thermocline water spreads uninhibited into the Banda, Flores, and Timor Seas and ultimately into the Indian Ocean. The model throughflow transport is about 7.0 Sv (Sv ≡ 10^6 m³ s⁻¹) in August 1993 and 0.6 Sv in February 1994, which is low compared to observationally based estimates. However, during the prolonged El Niño of the early 1990s the throughflow is suspected to be lower than average and, indeed, the model transports for the non–El Niño months of August 1988 and February 1989 are larger. It is likely that aspects of the model bathymetry, particularly that of the Torres Strait, which is too open to the South Pacific, and the Makassar Strait, which is too restrictive, may be the cause of the discrepancies between observations and model.

1. Introduction

The magnitude and variations of the Pacific to Indian Ocean Throughflow within the Indonesian Seas are considered to be key elements in the thermohaline balance of the Indian and Pacific Oceans (MacDonald 1993) and perhaps to the global climate system (Gordon 1986). Local variability of the Indonesian Seas may influence ENSO by governing the transfer of the warm tropical water between the Pacific and Indian Oceans (Wyrtki 1989; Tourre and White 1995). Furthermore, advective and tidal-induced mixing may influence the SST and sea–air coupling, with feedback on ENSO (Ffield and Gordon 1996; Godfrey 1996).

The interocean pressure gradient driving the Indonesian Throughflow is primarily confined to the upper 300 m of the water column (Wyrtki 1987). Observations indicate that within this layer the throughflow is composed mostly of North Pacific thermocline and intermediate water flowing through Makassar Strait (Fine 1985; Ffield and Gordon 1992; Bingham and Lukas 1994; Fieux et al. 1994; Gordon et al. 1994; Ilahude and Gordon 1996; Gordon and Fine 1996). In the deep channels east of Sulawesi, South Pacific water infiltrates the lower thermocline and dominates the deeper layers, including the overflow into the deep Banda Sea (van Aken et al. 1988; Gordon 1995; Ilahude and Gordon 1996; Gordon and Fine 1996; Hautala et al. 1996).

Corresponding author address: Prof. Arnold Gordon, Lamont-Doherty Earth Observatory, Columbia University, Palisades, NY 10964-8000.
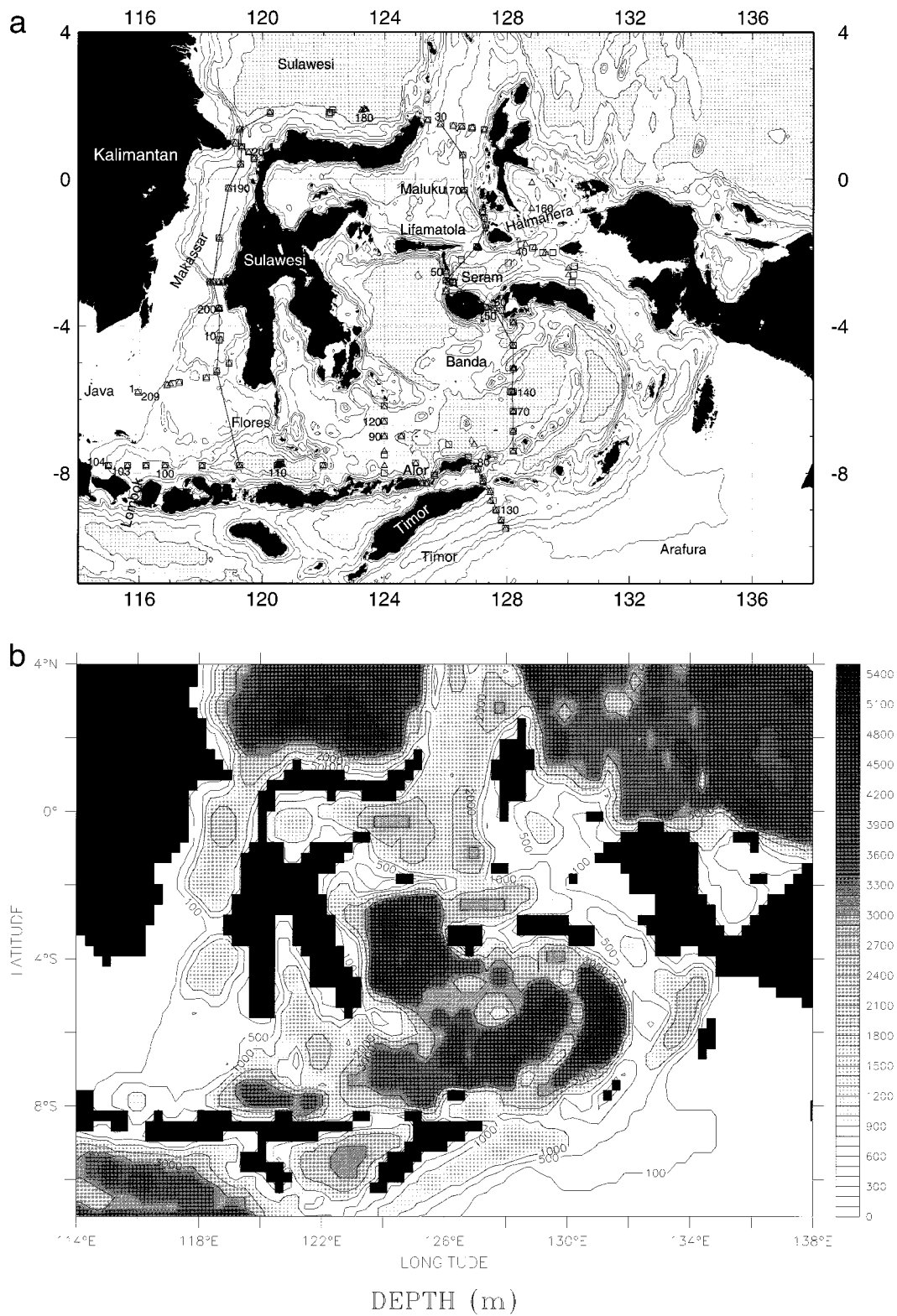E-mail: agordon@ldeo.columbia.edu

FIG. 1. (a) Bathymetry of the deep Indonesian Seas. The symbols indicate the positions of the Arlindo CTD stations. The 100-, 200-, 500-, 1000-, 2000-, 3000-, and 4000-m isobaths are shown, as are the seas and other features referred to in the text. The stations composing the three sections presented in Figs. 2, 3, and 4 are also displayed. (b) Model bathymetry of the Indonesian Region showing the 500-, 1000-, 2000-, 3000-, and 4000-m isobaths.
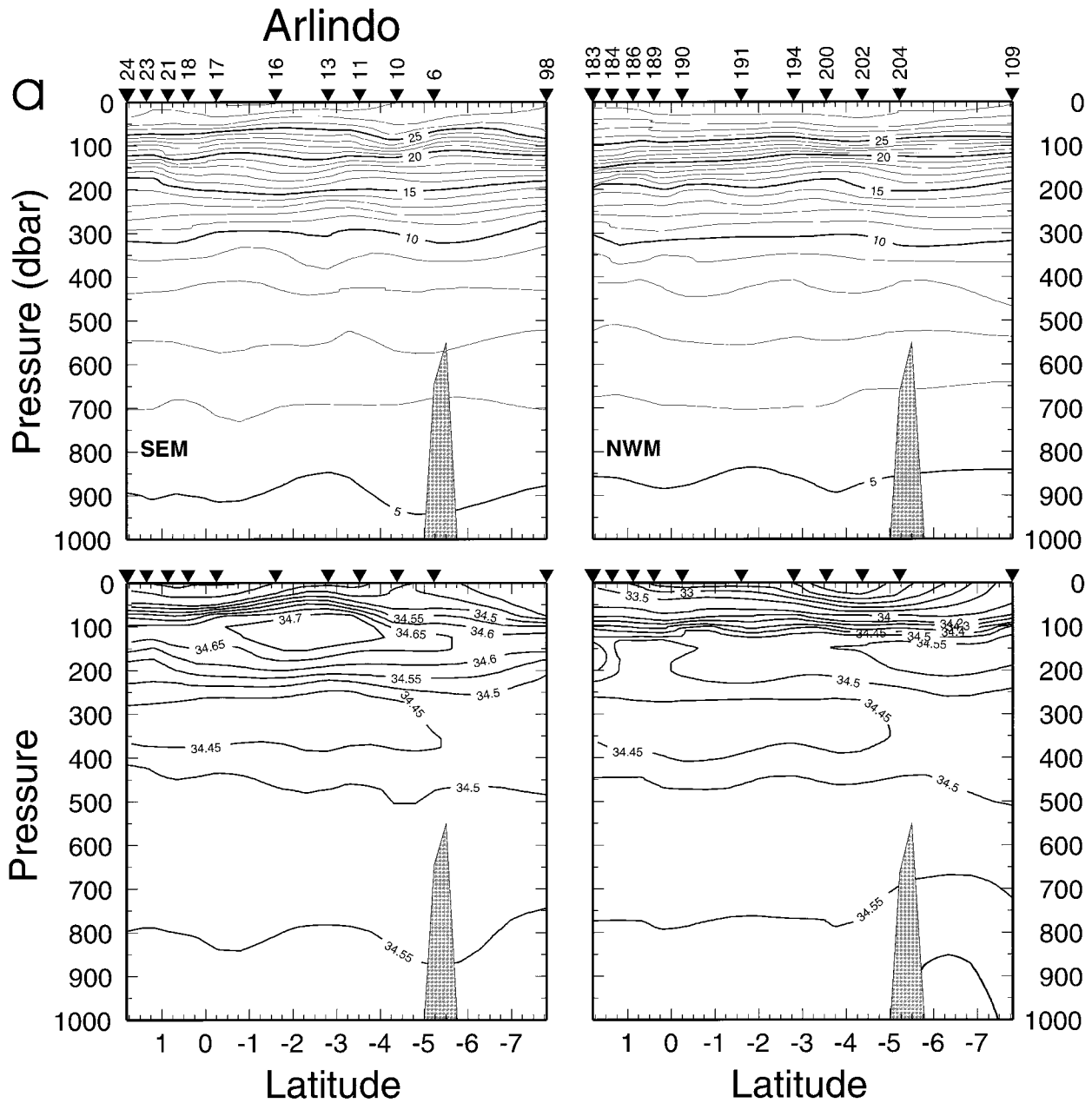
FIG. 2. Makassar section (see FIG. 1a) of potential temperature and salinity for the upper 1000 dbar. SEM represents the southeast monsoon of August 1993; NWM represents the northwest monsoon of February 1994. (a) Observational data, the bottom feature shown at 5° to 5.5°S is the observed shallowest sill encountered along the Makassar section; (b) model output, the same bottom depths as used in (a); these are based solely on the depths at the Arlindo station sites.

While some Makassar transport flows through the Lombok Strait, most passes through the Flores Sea into the Banda Sea. Here it is joined by additional transport derived from the deep eastern throughflow channels and then enters the Indian Ocean by way of the passages on either side of Timor (regional geometry is shown in Fig. 1a).

Transport estimates based on observations, models, and conjecture range from near zero to 30 Sv (Sv $\equiv$ 10^6 m^3 s^{-1}: Wyrtki 1961; Godfrey and Golding 1981; Gordon 1986, Kindle et al. 1989; Murray and Arief 1990; MacDonald 1993; Cresswell et al. 1993; Hirst and Godfrey 1993; Miyama et al. 1995; Molcard et al. 1994; Molcard et al. 1996). Measurements in the Lombok Strait from January 1985 to January 1986 (Murray and Arief 1988; Murray et al. 1989) show an average transport of 1.7 Sv with a maximum of 3.8–4.0 Sv toward the Indian Ocean during July and August. A min-
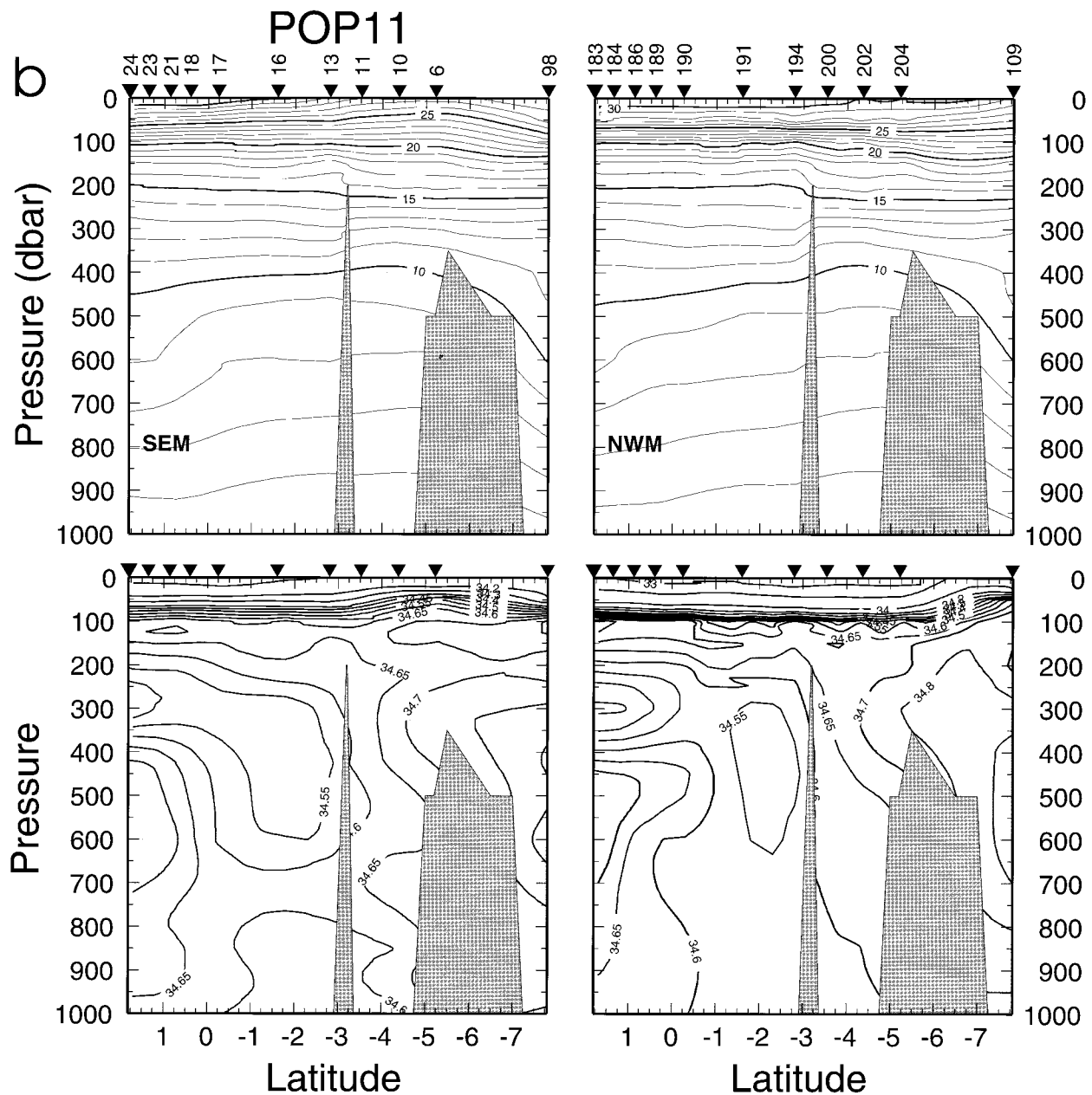
FIG. 2. (*Continued*)

imum between zero and 1 Sv, also toward the Indian Ocean, is observed from December 1985 to January 1986. The most recent observational-based estimates of transports through the Timor Sea are 18.6 Sv for August 1989 (Fieux et al. 1994) and −2 Sv (flow toward the Pacific Ocean) during February–March 1992 (Fieux et al. 1996), denoting the seasonal cycle. However, as Fieux et al. (1996) stress, interannual variability cannot be ruled out, noting that the February–March 1992 period falls within an El Niño episode. Meyers et al. (1995) estimated the annual mean flow to be 5 Sv through the upper 400 m across a section between Java and Australia

from XBT data for the period 1983–89, with a 12 Sv August–September maximum, and essentially zero transport in May–June and again in October–November. Meyers (1996), Fieux et al. (1996), and Gordon and Fine (1996) all suggest that the throughflow is reduced during El Niño episodes when sea level stands lower at the tropical Pacific entrance to the Indonesian seas. Molcard et al. (1996), using two moorings between Roti Island and Ashmore Reef (March 1992–April 1993), estimate a mean transport of 4.3 Sv between the sea surface and 1250 m in the Timor Passage, the deepest of the exit passages to the Indian Ocean. Of this trans-
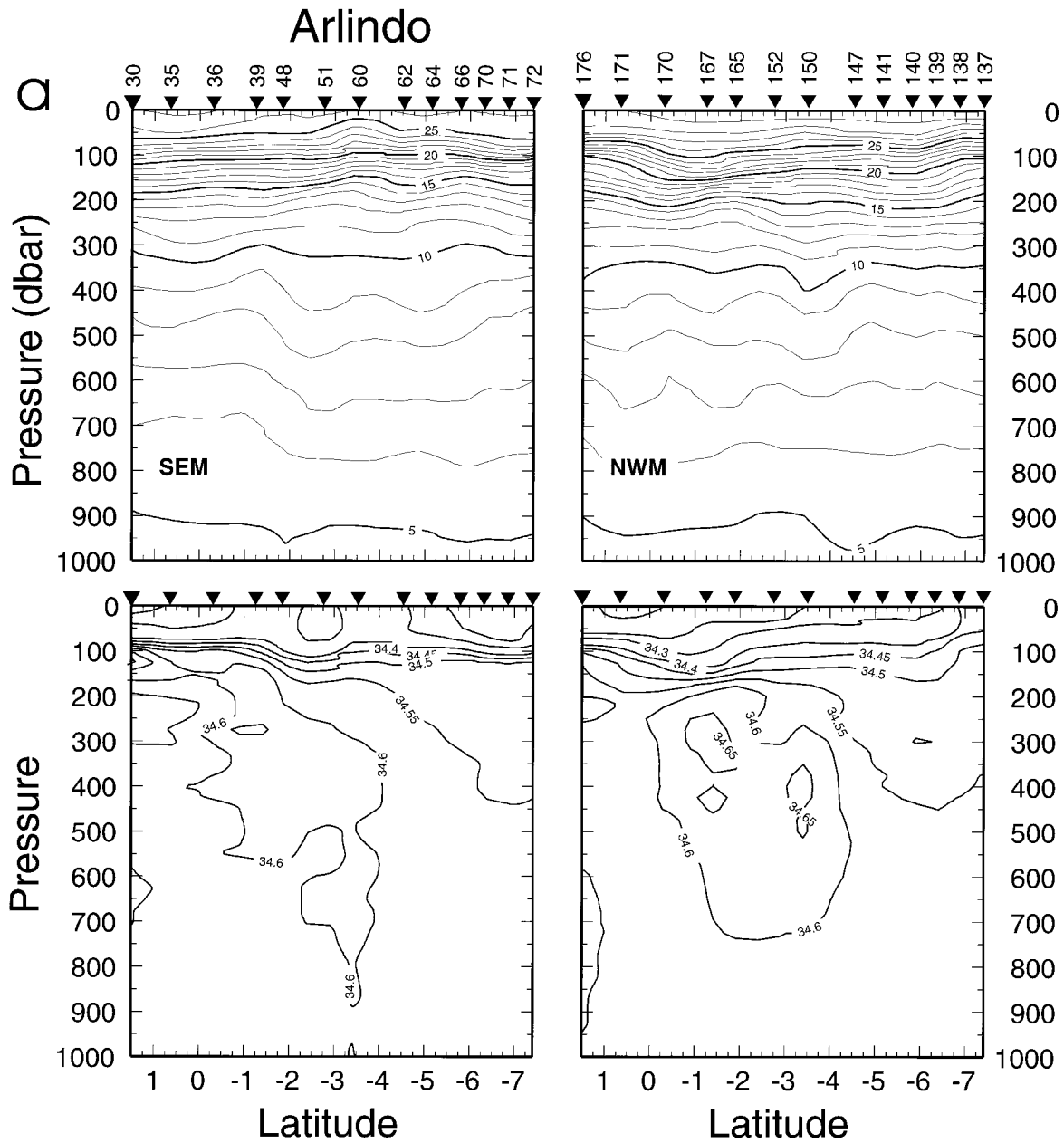
FIG. 3. Maluku–Seram–Banda section (see Fig. 1a) of potential temperature and salinity for the upper 1000 dbar. SEM represents the southeast monsoon of August 1993; NWM represents the northwest monsoon of February 1994. (a) Observational data; (b) model output.

port 1.8 Sv is confined to depths below the thermocline, between 400 and 1250 m, and may be representative of the South Pacific component of the throughflow. Density-driven overflow of South Pacific water into the deep Banda Sea across the Lifamatola Passage (sill depth 1940-m) contributes approximately 1.5 Sv to the total throughflow (Broecker et al. 1986; van Aken et al. 1988; van Bennekom 1988).

Thus, "prevailing wisdom" seems to point to 5–10 Sv annual average throughflow, with the maximum transport occurring during the southeast monsoon (Au-

gust). Interannual modulation by ENSO may account for as much as a 5 Sv reduction in transport (Meyers 1996).

For global models to faithfully reproduce the earth's climate system, interocean fluxes of mass, heat, and freshwater must be properly represented. The Indonesian Seas with their complex topography, located near the division of the North Pacific and South Pacific water mass fields, represent a severe challenge to model validity. The objective of this paper is to compare thermohaline stratification and water spreading patterns as
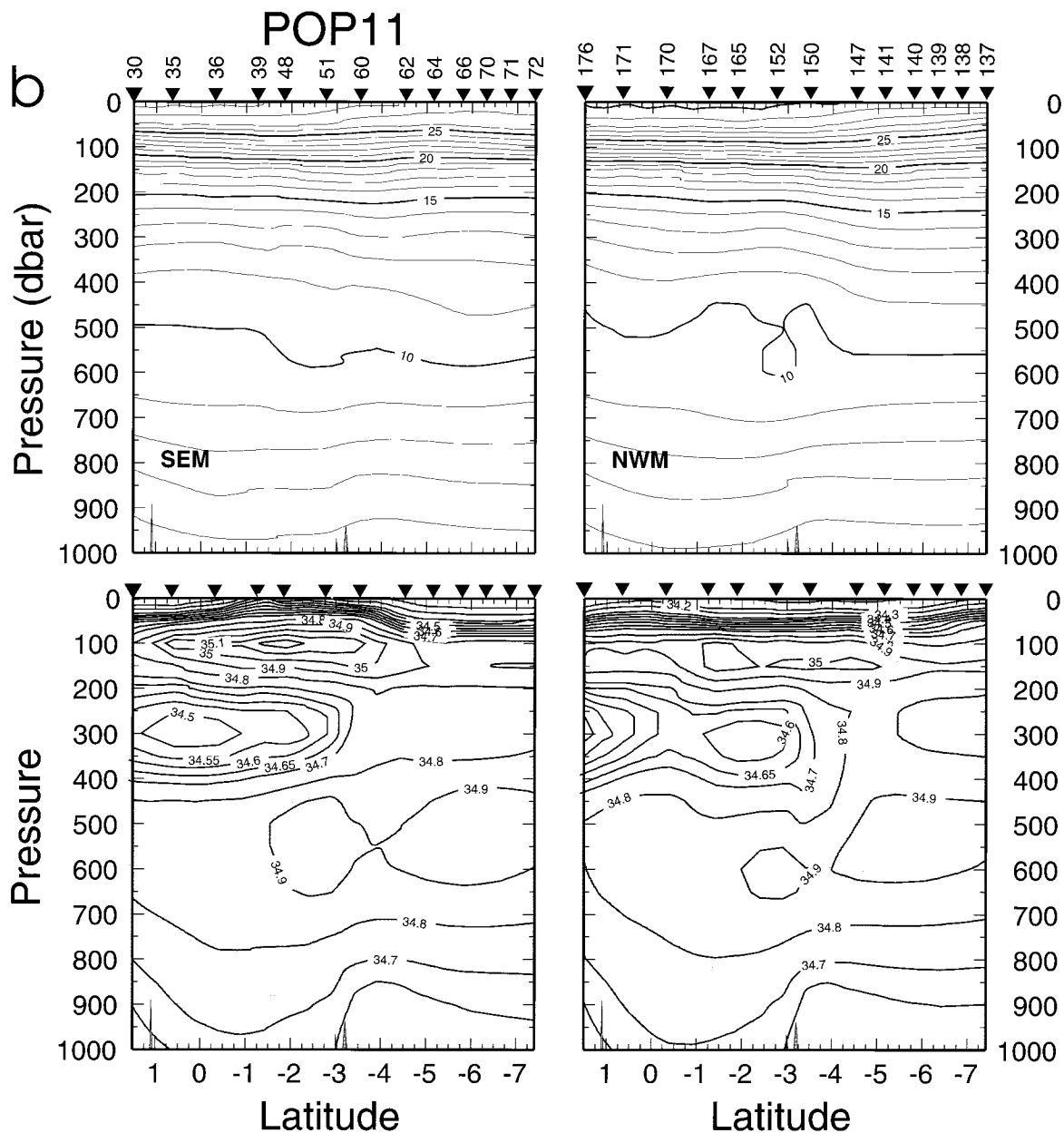
FIG. 3. (*Continued*)

seen in observations made in 1993 and 1994 with the results of the Los Alamos Parallel Ocean Program 1/6 deg global model.

2. Arlindo observations

The first phase of the Arlindo Project (a joint oceanographic research endeavor of Indonesia and the United States) consists of an extensive suite (Fig. 1a) of CTD measurements extending to the sea floor or to 3000 decibars obtained from the Indonesian Research Vessel *Baruna Jaya I* during the southeast monsoon (SEM) of 1993 (6 August–12 September) and northwest monsoon

(NWM) of 1994 (25 January–3 March). During this period the Southern Oscillation index remained negative, representing a rather prolonged, though mild El Niño episode.

3. Model description

The numerical simulation used in this paper is the Los Alamos National Laboratory (LANL) Parallel Ocean Program (POP) global ocean model. It is an eddy-resolving, 20-level, primitive equation model configured for a one-sixth degree (on average) Mercator grid. It was initialized from a net, 35-yr spinup from Levitus
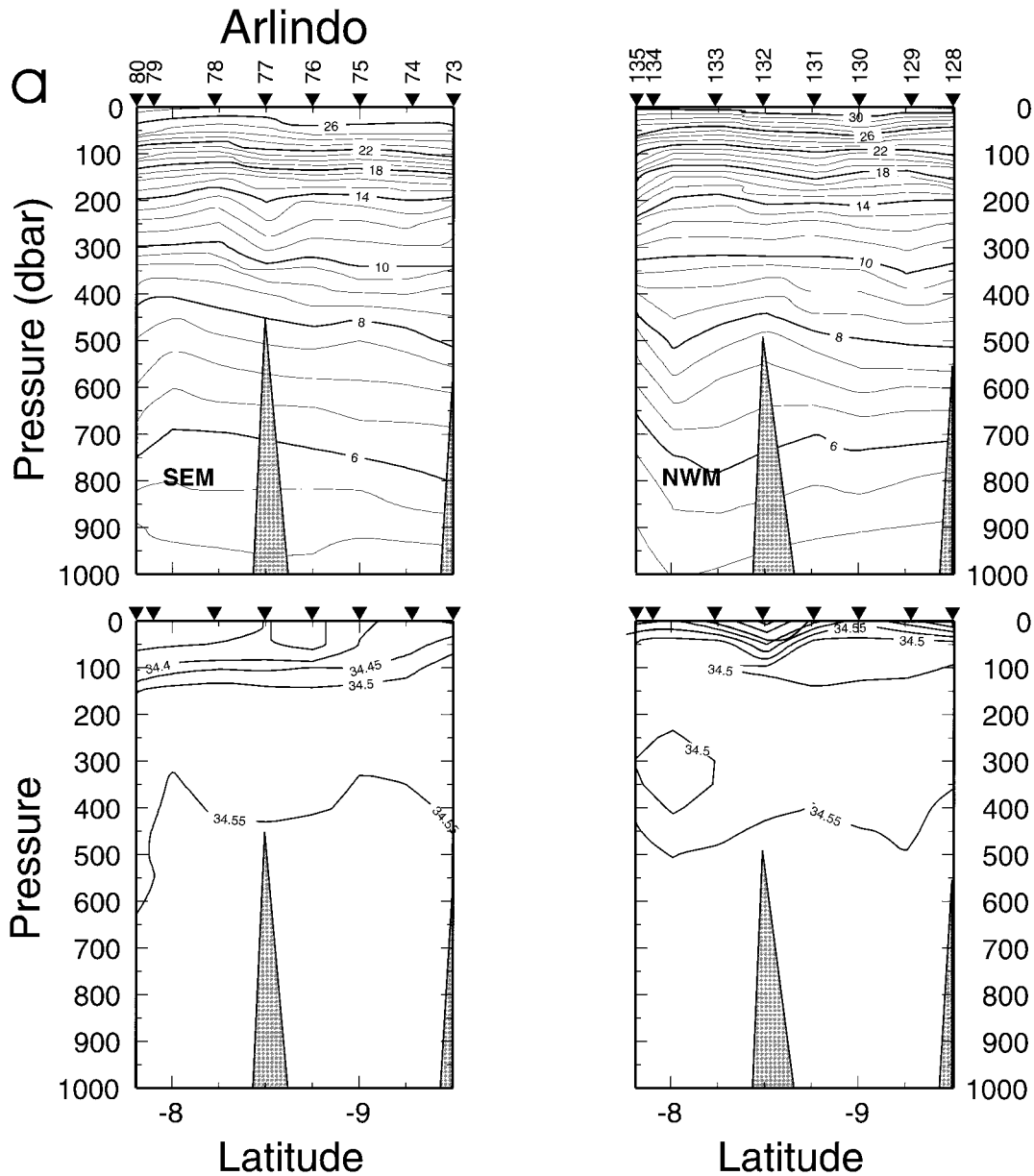
FIG. 4. Timor section (see Fig. 1a) of potential temperature and salinity for the upper 1000 dbar. SEM represents the southeast monsoon of August 1993; NWM represents the northwest monsoon of February 1994. (a) Observational data; (b) model output.

(1982) at lower resolution, followed by 25 years at the same resolution. Monthly climatological surface heat fluxes obtained from European Center for Medium-Range Forecasts (ECMWF) analyses (Barnier et al. 1995) and daily ECMWF wind stresses averaged to three days were used to force the model. The surface salinity was restored to Levitus (1982) monthly climatology with a restoring timescale of 30 days and the topography is ETOP05. Further details of the model formulation can be found in Fu and Smith (1996), McClean et al. (1997), and Maltrud et al. (1998).

4. Comparison of observational and model data

An array of monthly averaged model temperature and salinity values for August 1993 and February 1994, interpolated to coincide with the positions of the Arlindo CTD stations, is compared to the Arlindo observational results along three sections during each monsoon season: the western throughflow channel along the Makassar Strait (Fig. 2) and along the eastern throughflow channel from the Maluku to the Banda Seas (Fig. 3). The third section crosses the Timor Sea (Fig. 4), the major outflow of Indonesian water into the Indian
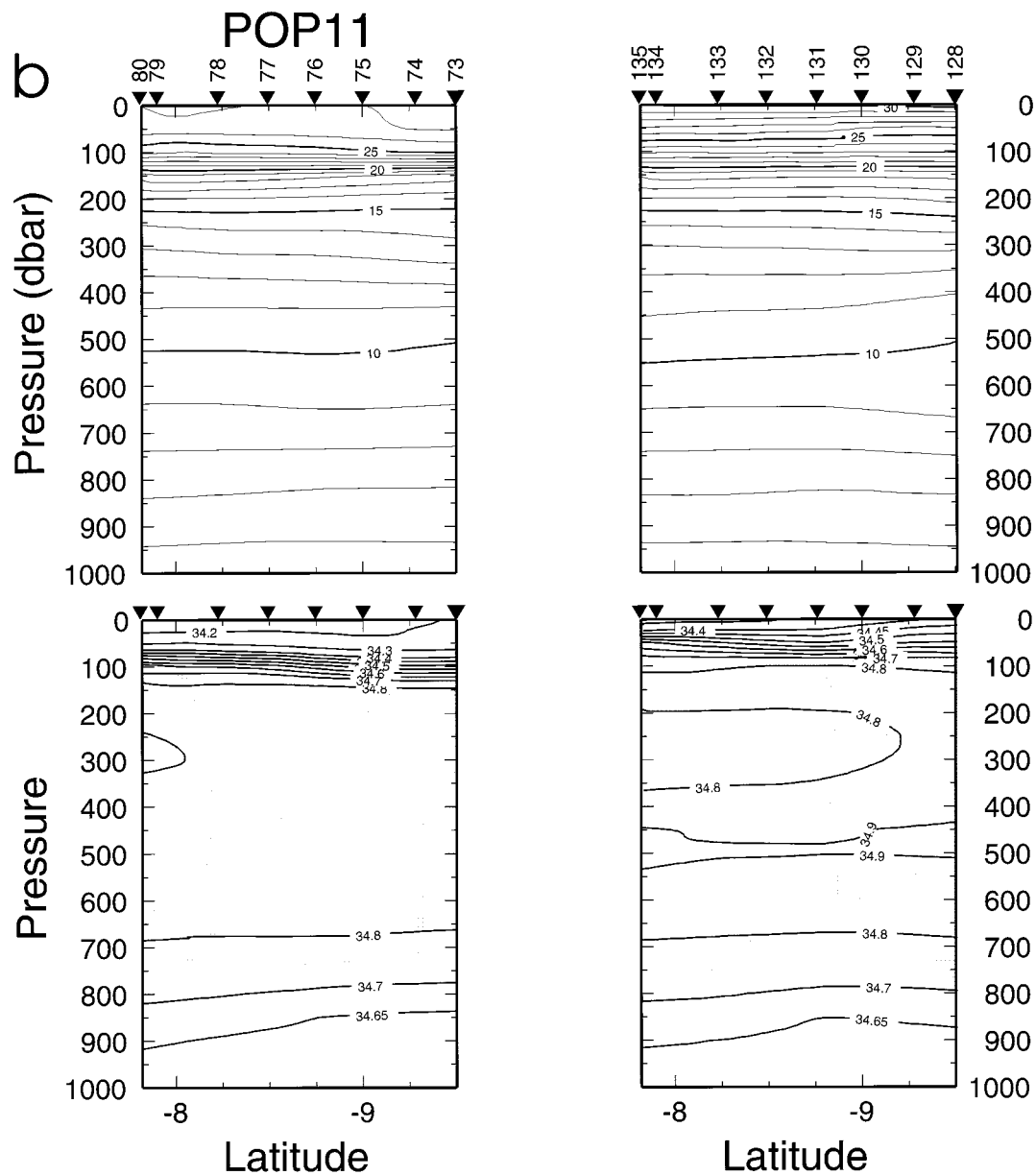
FIG. 4. (*Continued*)

Ocean. The three sections correspond in each case to a full line joining stations in Fig. 1a; each observed and corresponding model section have been projected onto a meridian for comparison purposes.

a. Potential and salinity sections

1) OBSERVATIONAL DATA FOR MAKASSAR SECTION

The western throughflow channel along the axis of the Makassar Strait (Fig. 2a) marks the primary throughflow route for North Pacific thermocline water. The temperature distribution reveals little variation with season. Water in excess of 25°C occurs within the upper 75 dbar;

the 10°C isotherm is near 320 dbar, and the 5°C isotherm falls between 800 and 900 dbar. The gradient between the 20° and 25°C isotherms is extremely sharp, as these isotherms are separated by less than 50 dbar. The salinity stratification displays seasonal changes. The surface salinity is much lower in the NWM, a response to greater precipitation and river runoff from Kalimantan. The subsurface salinity maximum (S_{max}), which denotes the presence of North Pacific subtropical water, is more pronounced in the SEM, suggesting greater throughflow of North Pacific thermocline water (to counter the effects of vigorous vertical mixing characteristic of that region) of the S_{max} core in that season. The salinity minimum

(S_{min}) near 300 dbar marks intrusion of North Pacific Intermediate Water.

2) MODEL DATA FOR MAKASSAR SECTION

The model salinity stratification along the Makassar Strait (Fig. 2b) differs from the observations, particularly below 150 dbar. The salinity in the northern Makassar Strait goes awry below the S_{min} of the North Pacific Intermediate Water, attaining values above 34.6. The S_{min} does not spread south of the midpoint of the strait near 3°S. This depth interval is replaced to the south by very saline water, reaching over 34.8 psu, well above observed values. Part of this difference is attributed to the model bottom topography. Near 3°S the model has a very narrow passage (one longitudinal grid box wide in velocity—0.28°) with a 200-m sill (Fig. 1b), whereas the observations show a wider, much deeper (Fig. 1a) channel at that site. The observed controlling sill is 550 m deep at 5.5°S (Gordon et al. 1994). The model's narrow, shallow sill blocks Makassar water from passing into the Flores Sea, which is then dominated by inflow from the Banda Sea.

The model water column below 200 dbar is warmer than the observed water column, indicating more stored heat in the model field. The model density (not shown) is dominated by the temperature and so is less dense than the observations from 200 to 1200 dbar. In general, the model thermocline is thicker (more diffuse) than the observed thermocline, most likely a consequence of the model's vertical mixing scheme. This behavior has been observed in models in which constant vertical mixing coefficients are used (Bryan 1987; Schott and Böning 1991). While the Richardson-number-dependent parameterization used in the POP model tends to alleviate this problem (Pacanowski and Philander 1981), an isopycnal mixing formulation may be more appropriate (R. Bleck 1996, personal communication).

Another cause for the model/data discrepancies may be due to the lack of a tidal mixing parameterization in the POP model. Ffield and Gordon (1992) attribute the attenuation of the North Pacific subsurface S_{max} (near 100 dbar) to tidal mixing. Since the salinities in the southern Makassar channel of the model are all too high, the inclusion of tidal mixing is unlikely to produce more than a minor improvement to the salinity stratification. A major response would result from incorporating more realistic topography in the Makassar Strait.

3) OBSERVATIONAL DATA FOR THE MALUKU TO BANDA SEA SECTION

The salinity field along the eastern channel reveals (Fig. 3a) that the North Pacific S_{max} and S_{min} occurs only in the Maluku Sea (1.5°N–0.5°S). In the Seram and northern Banda Seas (2°–3.5°S), the S_{max} near 20°C is absent. Instead, a deeper colder S_{max} derived from the South Pacific lower thermocline is observed. This water

enters the Seram Sea from the Halmahera Sea across a 500-m sill (Fig. 1a). In the southern Banda Sea (3.5°–7.5°S) the similarity of the thermocline characteristics with those of the Flores Sea reflect the circulation link with Makassar Strait.

The observations reveal that during the NWM the thermocline is deeper than during the SEM in the region extending from the Seram Sea to the central Banda Sea (1°–4°S); the average seasonal change in depth is approximately 40 dbar. In the Banda Sea, observed sea surface temperature during the SEM is about 4°C colder than during the NWM. Seasonal heaving of the thermocline and seasonality of the SST in the Banda and Seram Seas are associated with strong seasonal wind forcing, inducing SEM surface water divergence and NWM convergence (Wyrtki 1961).

4) MODEL DATA FOR THE MALUKU TO BANDA SEA SECTION

The model and observed salinity fields differ significantly; the sharp model halocline between 25 and 50 dbar and the high salinity (greater than 35) of the 20°C water near 100 dbar (Fig. 3b) are not observed in the Arlindo data (Fig. 3a). The S_{max} layer around 100 dbar is far more saline than the S_{max} subtropical underwater of North Pacific water and is closer to the South Pacific S_{max} subtropical underwater. It is likely that in the model the South Pacific S_{max}, drawn from the New Guinea Coastal Undercurrent, is introduced into the Seram and adjacent seas from the Halmahera Sea. This does not seem to be a sill depth problem, as 100 dbar is well above the observational and model sill depth of the Halmahera Sea.

The S_{min} of the North Pacific Intermediate Water (NPIW) in the model is more pronounced and penetrates farther into the Banda Sea than revealed in the observations. The North NPIW signal is still apparent in the model Timor Sea and hence represents a contrast to the generally weaker North Pacific thermocline presence within the model. At depths below the S_{min} the model salinity is again well above that of the observations. The saline layer greater than 34.8 psu between 500 and 700 m is too salty to be derived from the North Pacific although too deep to be derived solely from the Halmahera Sea (model sill is slightly less than 500 m, Fig. 1b). It may result from mixing in roughly equal amounts of the downwelled South Pacific S_{max} within the Banda Sea and upwelled deeper Banda Sea water, perhaps with some input from the Indian Ocean.

As found in the Makassar Strait the model water column temperature (Fig. 3b) below the depth of the 20°C isotherm is warmer than the observational data, presumably a result of the vertical mixing scheme. The model thermal stratification along the eastern channel has a 20-m seasonal change in thermocline depth and a 2°C seasonal change in SST, both about half of the seasonal variability seen in the observations.

5) OBSERVATIONAL DATA FOR THE TIMOR SEA SECTION

In the Timor Sea, the observations (Fig. 4a) display a thermocline stratification characteristic of the southern Banda Sea, which in turn is similar to that found in the Flores Sea and Makassar Strait, a natural consequence of the flow pattern. The warmer, salty surface water observed during the NWM and the cooler, fresher surface water of the SEM are a response to local sea–air fluxes.

6) MODEL DATA FOR THE TIMOR SEA SECTION

As expected, the model data (Fig. 4b) mirrors the model Banda Sea, which is far more saline than the observed Banda Sea. The model S_{min} near 300 dbar indicates a surviving trace of North Pacific Intermediate Water, a trait not as clearly marked within the observations. The NWM surface water in the model is very warm, in excess of 30°C approximating the observed SST, but the corresponding high surface salinity is not modeled. A major model–data difference is found where water is colder than 4°C. The observed data reveal an intrusion of a deep saline layer from the Indian Ocean below the observed 1200-m sill depth within the Banda Sea (Fieux et al. 1994); this feature is not seen in the model fields.

b. Circulation and transport

The Arlindo observations were used to determine the water-mass spreading pattern of the thermocline (Gordon and Fine 1996). This pattern does not portray an instantaneous or monthly circulation but rather is a response to the advective and diffusive processes averaged over a period of the residence time, estimated as six months to 1 yr (Ffield and Gordon 1992). Deeper water mass spreading patterns, discussed by van Aken et al. (1988) and van Bennekom (1988) based on the *Snellius II* data, reflect a longer residence timescale, spanning a decade or more. The model velocity and transport fields are monthly averages, so total similarity is not expected with the water-mass-derived circulation in a time-varying regime. With this limitation in mind, we next relate the throughflow patterns of the upper 1000 m deduced from the Arlindo data for August 1993 and February 1994 with POP transport values for these months.

1) VELOCITY

The reversal of the model surface flow (12.5 m: Figs. 5a,b) in response to the monsoon wind forcing is apparent and, for most areas, is in very good agreement with the climatic mean surface current fields presented by Wyrtki (1961). In August 1993 (Fig. 5a) the POP surface water flows westward across the Banda Sea, through the Flores Sea, and into the Java Sea in response

to the southeast wind. Southward flow across 2°–47°S is shown in the Seram Sea and in Makassar Strait. The northward flow along the western edge of the Makassar Strait lying over shallower water (100–500 m: Fig. 1) is not corroborated by the Wyrtki current map. Strong westward flow crosses the Arafura Sea after flowing through the Torres Strait, a shallow passage between Australia and New Guinea along 142°E (not shown in figure). Surface water passes southward into the Indian Ocean through the major channels (Lombok and Alor) of the Sunda Island chain. Eastward flow marking the South Java Current curls to the south to join the throughflow south of Java. With the exception noted, these velocity patterns are all seen in Wyrtki (1961).

In February 1994 (Fig. 5b) the surface flow is nearly opposite to that of August 1993. Eastward flow from the Java Sea advects into the Flores Sea, is augmented by northward flow from Lombok Strait, and then passes into the Banda Sea. The South Java Current is present in both seasons, but in February 1994 it extends farther to the east feeding the northward flow through Lombok Strait rather than turning southward to join the throughflow. Surface water flows northward in the Makassar Strait, in opposition to the Makassar surface currents shown by Wyrtki (1961). Another discrepancy with the Wyrtki map is in the Halmahera Sea, where Wyrtki shows northward flow, and the model shows southward flow. Northward and eastward flow of surface water, derived from the southern boundary (south Indian Ocean), is modeled east of Timor, extending into the Torres Strait.

The flow at 117.5 m (Figs. 5c,d) reflects the thermocline circulation, near the S_{max} core layer. There are a number of differences with the deduced flow pattern based on the observed water-mass distribution discussed by Gordon and Fine (1996). The POP velocities at 117.5 m for August 1993 (Fig. 5c) are directed toward the south in the Makassar Strait, drawn from the Mindanao Current, consistent with the presence of North Pacific S_{max} subtropical water. The New Guinea Coastal Current (2°S–2°N, 115°–140°E) advects South Pacific thermocline water toward the Halmahera Sea with a weak branch continuing into the Seram Sea, which joins a stronger southward flow from the Maluku Sea extending along the western Banda Sea. The western Banda flow converges with northward flow to feed an eastward current between 4° and 5°S.

Flow is directed into the Banda Sea from the Timor Passage, part of which is redirected to the Indian Ocean within the Alor Passage and Lombok Strait. This flow pattern is not in agreement with the water mass observations, which suggest eastward flow of thermocline water in the Flores sea with export to the Indian Ocean both north and south of Timor. However, the water-mass-based flow patterns may not fully reflect subbasin-scale recirculation cells.

The February 1994 flow at 117.5 m (Fig. 5d) displays some differences from the August 1993 model field.

(a)

AUGUST, 1993
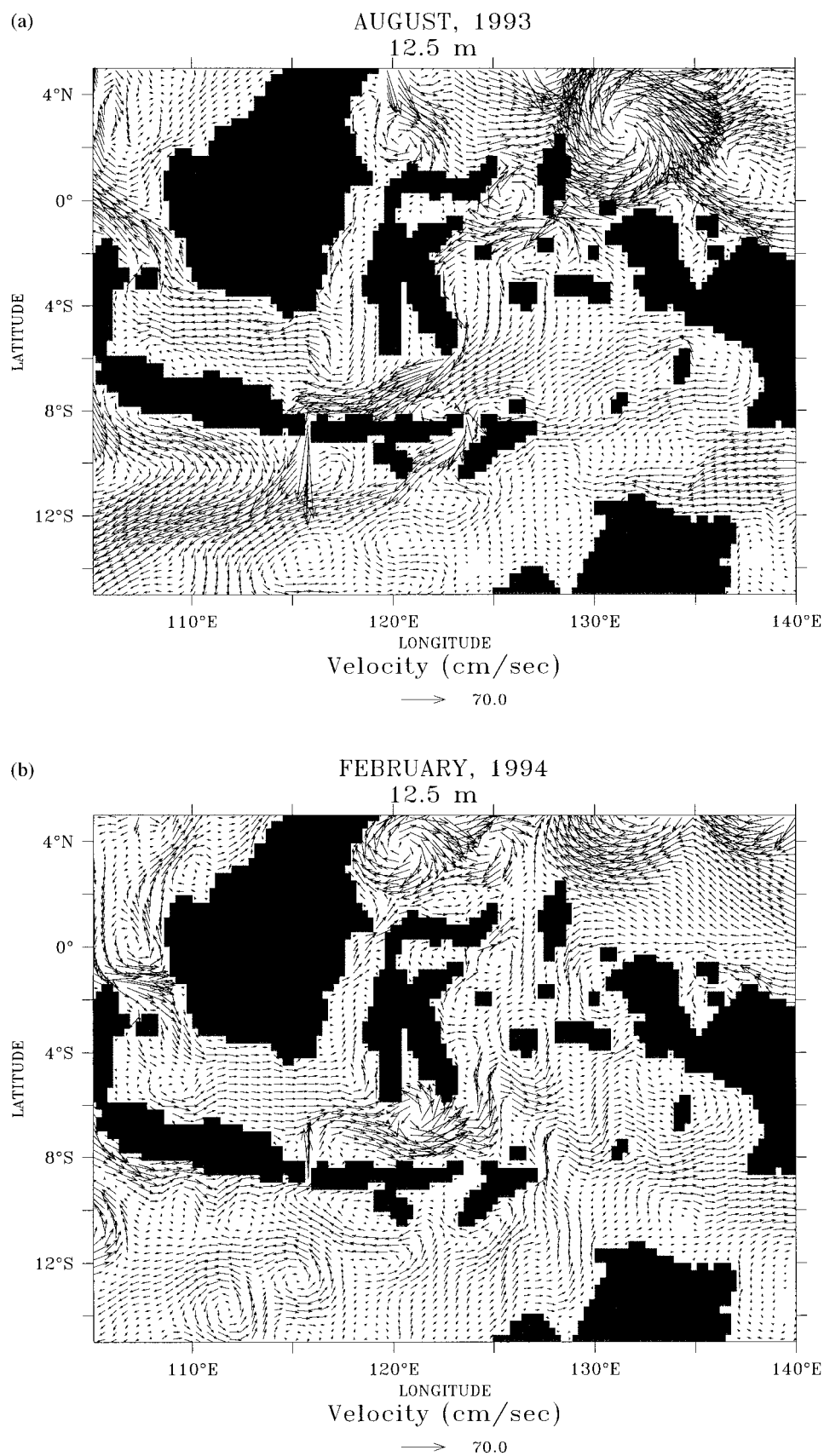12.5 m

(b)

FEBRUARY, 1994
12.5 m

FIG. 5. Horizontal velocity from the model at the 12.5 m, (a) and (b), and at 117.5 m, (c) and (d), for the periods of the two Arlindo CTD cruises: August 1993 representing the southeast monsoon and February 1994 representing the northwest monsoon.
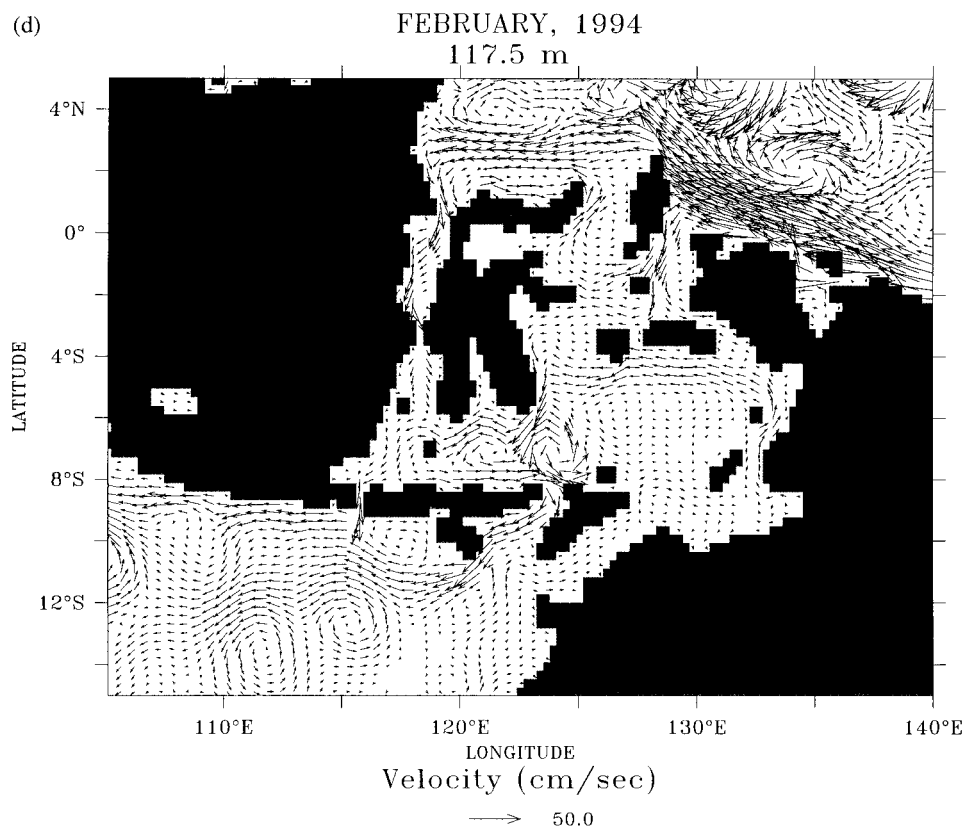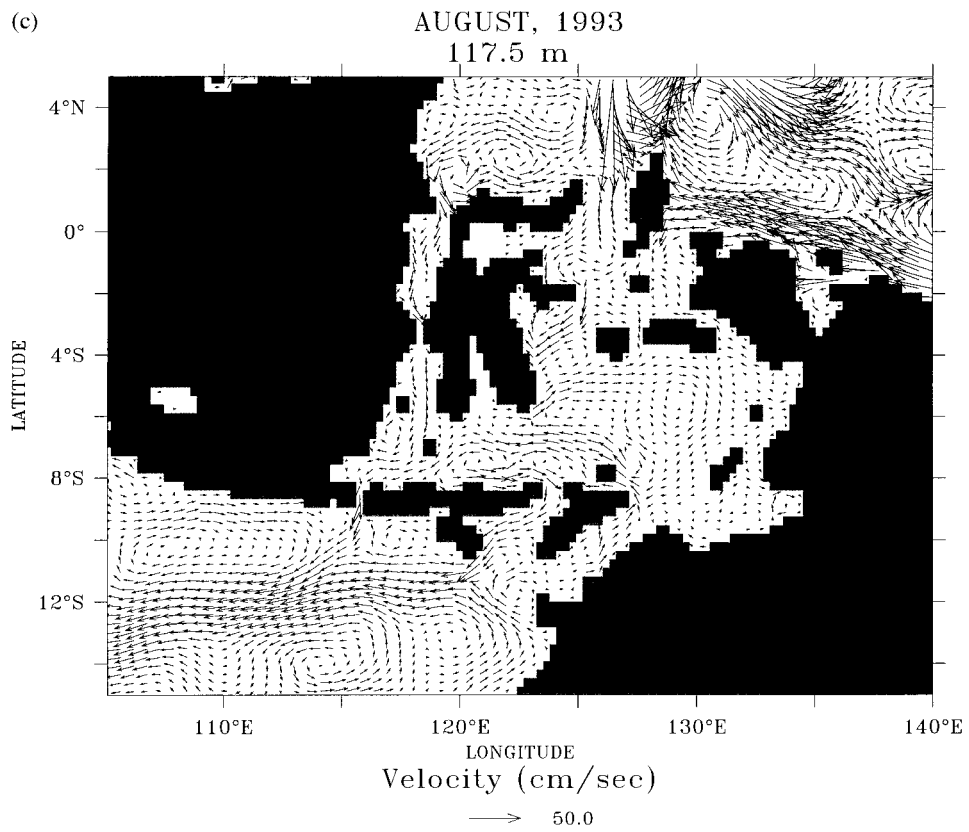
(c)

AUGUST, 1993
117.5 m

Velocity (cm/sec)

⟶ 50.0

(d)

FEBRUARY, 1994
117.5 m

Velocity (cm/sec)
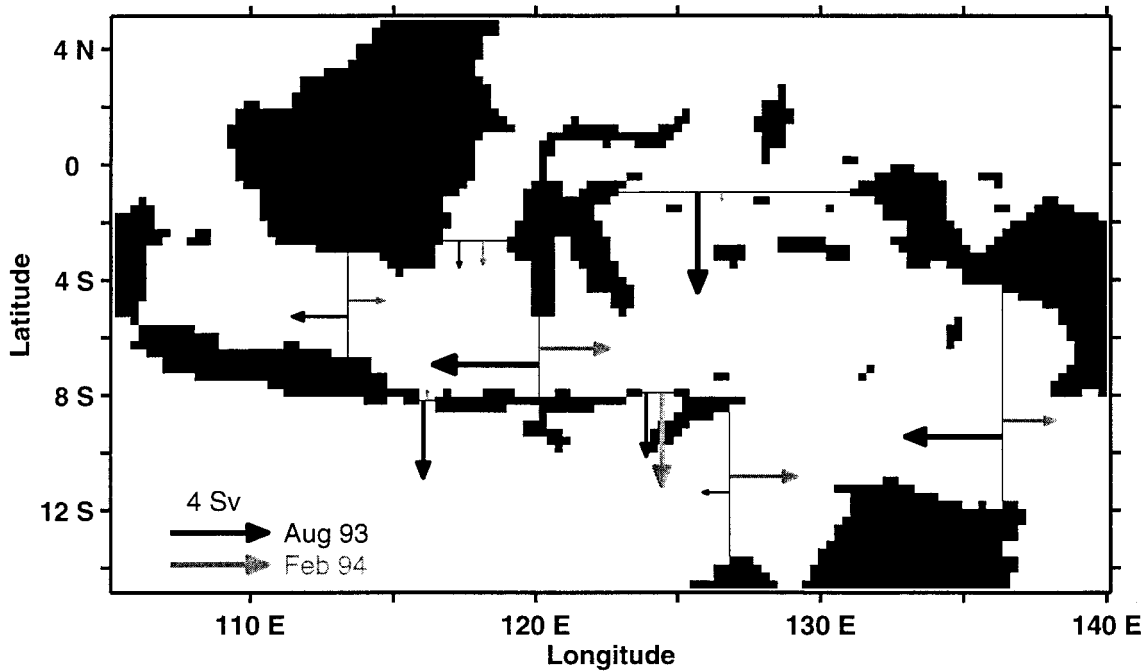
⟶ 50.0

FIG. 5. (*Continued*)

FIG. 6. Transport in Sverdrups across various passages within the Indonesian seas. The solid arrows denote August 1993; the gray arrows denote February 1994. The values are provided in Table 1.

Stronger flux from the Halmahera to the Seram Sea is seen. The Halmahera inflow diverges, feeding northward flow along the western margin of the Maluku Sea, with a weaker southward branch along the western margin of the Banda Sea. Within the western Banda Sea the Seram Sea influx combines with a westward zonal flow along 5°S, which is derived from the Indian Ocean inflow south of Timor, to contribute to the export in the Alor and Lombok Passages. The zonal flow in the model is fed by strong vertical advection in the eastern Banda Sea (figure not shown).

2) TRANSPORTS

The model transports across select passages (Fig. 6; Table 1a,b) show year round flow toward the Indian Ocean: 7.0 Sv during the 1993 SEM and 0.7 Sv during the 1994 NWM, yielding a 3.9 Sv average. Seasonal variability is found by observations (Molcard et al. 1994; Molcard et al. 1996; Meyers et al. 1995), although observationally based throughflow annual average estimates are slightly larger. For example, the August 1989 and February 1992 Timor Sea average is 8.3 Sv (Fieux et al. 1994; Fieux et al. 1996), the XBT-based estimate by Meyers et al. (1995) is 5 Sv, and a 6.0 Sv total is obtained by summing the current meter mooring values in the Timor Sea (Molcard et al. 1996) and Lombok Strait (Murray and Arief 1989). The Alor Passage transport is not included in these estimates. The model Lombok Strait transport values of 3.2 Sv toward the Indian Ocean in August 1993 and 0.4 Sv toward the north in February 1994 can be considered to be in excellent agreement with the 1985/86 measurements (Murray and Arief 1989). Flow toward the Indian Ocean through shallow passage between Java and Sumatra and between Sumatra and Singapore may provide an addition 1 Sv (Piola and Gordon 1984).

In August 1993 the primary model paths introducing Pacific water into the Indonesian seas are across the

TABLE 1a. Model total transports (in Sverdrups) during the Arlindo field observations, Aug 1993 and Feb 1994. Negative values are westward or southward and positive values are eastward or northward.

Passage (Fig. 6)	Aug 93	Feb 94	Average
Lombok	−3.2	+0.4	−1.4
Makassar	−1.1	−1.0	−1.1
Sulawesi–Irian	−4.1	−0.3	−2.2
Flores	−4.4	+2.9	−0.8
Timor	−1.1	+2.8	+0.9
Alor	−2.7	−3.9	−3.3
Java	−2.3	+1.5	−0.4
Arafura	−4.0	+2.2	−0.9

TABLE 1b. Total throughflow transports (Sverdrups).

	Aug 93	Feb 94	Average
Outflow to Indian*	−7.0	−0.7	−3.0
Inflow from Pacific**	−7.0	−0.7	−3.9

* Outflow includes Lombok, Timor, and Alor Passages.
** Pacific inflow includes Makassar, Sulawesi–Irian, Arafura, minus Java.

TABLE 2a. Model total transports (Sverdrups) for Aug 1988 and Feb 1989. Negative values are westward or southward and positive values are eastward or northward.

Passage	Aug 88	Feb 89	Average
Lombok	−5.7	−2.1	−3.9
Makassar	−6.0	−0.6	−3.3
Sulawesi–Irian	−5.0	−2.2	−3.6
Flores	+1.2	+3.7	+2.5
Timor	−5.3	+0.6	−2.3
Alor	−7.2	−4.4	−5.8
Java	+0.9	+5.2	+3.0
Arafura	−6.3	+2.2	−2.0

TABLE 2b. Total throughflow transports (Sverdrups).

	Aug 1988	Feb 1989	Average
Outflow to Indian*	−18.2	−5.8	−12.0
Inflow from Pacific**	−18.1	−5.8	−12.0

* Outflow includes Lombok, Timor, and Alor Passages.
** Pacific inflow includes Makassar, Sulawesi–Irian, Arafura, minus Java.

Sulawesi–Irian Jaya (4.1 Sv) section and the Arafura shelf (4.0 Sv). The latter is derived from surface water transported across the shallow Torres Strait between Australia and New Guinea. The Makassar runs a poor third (1.13 Sv).

The model Torres Strait (the shallowest connection of the South Pacific to the Indonesian Seas between Australia and New Guinea, along 142°E) is 50 m deep and about 120 km wide. This is much deeper than the observed Torres Strait, which is less than 10 m deep with the presence of numerous islands and reefs. Based on 5 months of current observations, Wolanski et al. (1988) find strong tidal flow, but no evidence for mean flow through Torres Strait. Clearly the model allows too much communication across the Torres Strait. Simply removing the Arafura transport when considering the total throughflow may not be reasonable, as closing the model Torres Strait would alter the surface wind driven transport between the Arafura and Coral Seas as well as inducing unrealistic circulation patterns on either side of the Strait (A. Semtner 1996, personal communication). In addition, it may alter the transmission of the Coral Sea high pressure head into the southern Indonesian Seas, changing the access of the tropical Pacific water to the northern Indonesian seas via passages closer to the equator.

The depth distribution of the inflow is totally within the upper 360 m for the Makassar Strait and Arafura shelf passages. Across the Sulawesi–Irian Jaya passage, 4.6 Sv enters in the upper 360 m; between 300 and 985 m there is a northward flow of 3.0 Sv, and below 985 m, 2.6 Sv flows into the Indonesian seas. This latter flow probably includes the overflow of the Lifamatola Passage into the deep Banda Basin. The 3.0 Sv northward flow between 360 and 985 m consists of saline water apparent in the Maluku to Banda Sea model section (Fig. 3b). This transport may be derived from the return of upwelled deep Banda Sea water, mixing with warmer salty South Pacific subtropical underwater sinking from near 100 m (Fig. 3b). Some contribution of Indian Ocean water may be drawn from the model Alor and Timor Passages, which together show about a 0.9 Sv northward transport in the 360-m to 985-m layer (Alor is 1.3 Sv to the north, Timor is 0.4 Sv to the south).

In February 1994 the model throughflow into the Indian Ocean weakens to essentially zero (0.6 Sv). The Makassar Strait transport remains about the same as August 1993, but the Sulawesi–Irian Jaya transport drops to near zero. The (dubious) transport over the Arafura shelf reverses and is now directed toward the Coral Sea of the South Pacific Ocean. The Lombok Strait and Timor Sea transports are toward the north, into the Indonesian Seas. The main pathway of flow into the Indian Ocean is via the Alor Passage, which is slightly larger in February than in August. The transports below 360 m across the Sulawesi–Irian Jaya passage have reversed sign and are small: 0.3 Sv to the south in the depth range 360–985 m and 1.9 Sv to the north in water deeper than 985 m.

The model August 1993 transports show that the channels east of Sulawesi are the dominant throughflow pathways. The Torres Strait pathway is unlikely and probably an artifact of the excessively deep bathymetry in the model. In February 1994 the total interocean throughflow is essentially zero, with the Makassar Strait southward transport combined with the eastward flow in the Java Sea balancing the Torres Strait export to the South Pacific Ocean. The Alor Passage flow to the Indian Ocean is mostly compensated by northward flow within the Lombok Strait and Timor Sea.

3) INTERANNUAL TRANSPORT VARIATIONS

During 1993 and 1994 the Indonesian region was in the midst of a prolonged El Niño episode. The Southern Oscillation index (SOI) was negative from December 1989 to the middle of 1995. It is possible that the interocean throughflow during such periods may be lower than during a positive SOI (Meyers 1996), owing to the lower sea level at the Pacific entrance to the Indonesian seas. In order to test this possibility we compare model fields from August 1993 with those from August 1988 and February 1994 with those from February 1989 since the SOI was positive in 1998 and 1989 (Table 2)

The August 1988 throughflow is 18.2 Sv [agreeing nicely with the 1989 value of Fieux et al. (1994)], the February 1989 throughflow is 5.8 Sv, yielding an average of 12.0 Sv. These values are 2.6 and 8.8 times larger, respectively, than the corresponding months from 1993 and 1994. Additionally, the ratio of the transport through the various passages has changed: notably the Java and Flores transports are eastward for both months, the Lombok does not reverse sign, and the Makassar

displays strong seasonal variability. Also, in August 1988 the Makassar transport is somewhat larger than the southward transport in the Sulawesi–Irian Jaya passage. Clearly, interannual variability of the interocean transport associated with the ENSO phase may be as large as seasonal variability.

4) HEAT AND SALT FLUXES

To obtain a measure of the heat and salt transported between the Pacific and the Indian Oceans, fluxes of these properties were calculated from monthly averaged POP fields through a zonal section along 115°E between Australia and Java. Since this section lies west of Lombok Strait and the Indian Ocean basin farther north is closed, all throughflow water will cross this section. These calculations were made for the months coinciding with the Arlindo experiment (August 1993 and February 1994) and from August 1988 and February 1989 during the cold event in the Pacific basin.

The direct method of Hall and Bryden (1982) was used to calculate heat transports; however since the net volume transport across this section is not zero, these transports depend on the scale of temperature. Following Talley (1984) and Schneider and Barnett (1997) the transport is broken down into barotropic and baroclinic contributions where the barotropic term is referenced by the spatially averaged temperature of the return flow into the Pacific between Australia and Antarctica (2.8°C). It is written

$$\rho C_P \int \int u\theta \, dy \, dx = \rho C_P \int_0^L H(y)\overline{u}(\overline{\theta} - \theta_{\text{ref}}) \, dy$$

$$+ \rho C_P \int_0^L \int_0^{H(y)} u'\theta' \, dz \, dy$$

with

$$u = \overline{u} + u' \quad \text{and} \quad \theta = \overline{\theta} + \theta',$$

where $\overline{u}$ and $\overline{\theta}$ are depth-weighted averages of potential temperature and zonal velocity, θ_{ref} is the spatially weighted average of the return flow, and $H(y)$ is the ocean depth along the section.

The total heat transports in August 1993 and February 1994 are -0.79 and -0.06 PW (negative values are into the Indian Ocean), respectively. The barotropic contributions during these months are -0.09 and 0.12 PW, respectively, while the baroclinic components account for -0.70 and -0.18 PW, respectively.

The barotropic and baroclinic contributions were calculated for each month in 1993 and are shown in Fig. 7a and their totals are seen in Fig. 7b. A strong seasonal cycle is seen in the baroclinic flow (solid line), which is related to the seasonal cycle of the throughflow mass transport (Fig. 7c). The barotropic component (dashed line) is much smaller than the baroclinic component and lacks a season cycle. As previously noted, the model
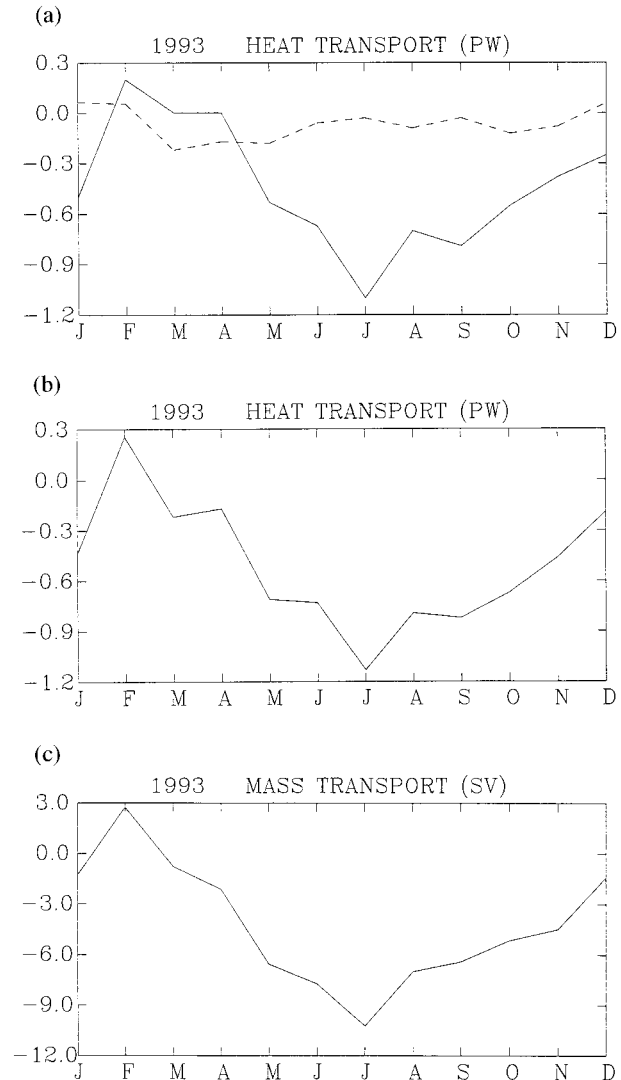

FIG. 7. (a) Baroclinic (solid line) and barotropic (dashed line) advective heat transports (PW), (b) total advective heat transport (PW), and (c) mass transport (Sv) across 115°E between Australia and Java for 1993.

throughflow transport was stronger during the 1988/89 period during a Pacific cold event. The total heat transport into the Indian Ocean was 1.77 and 0.64 PW in August 1988 and February 1989; both higher than the 1993/94 values.

As mentioned, the quantities used in the above calculation are $\langle u \rangle$ and $\langle \theta \rangle$, where angle brackets denote a monthly average. The total advective flux

$$\rho C_P \int \int \langle u\theta \rangle \, dz \, dy$$

is also archived, and the difference between it and the flux due to the mean currents,

$$\rho C_P \int \int \langle u \rangle \langle \theta \rangle \, dz \, dy,$$
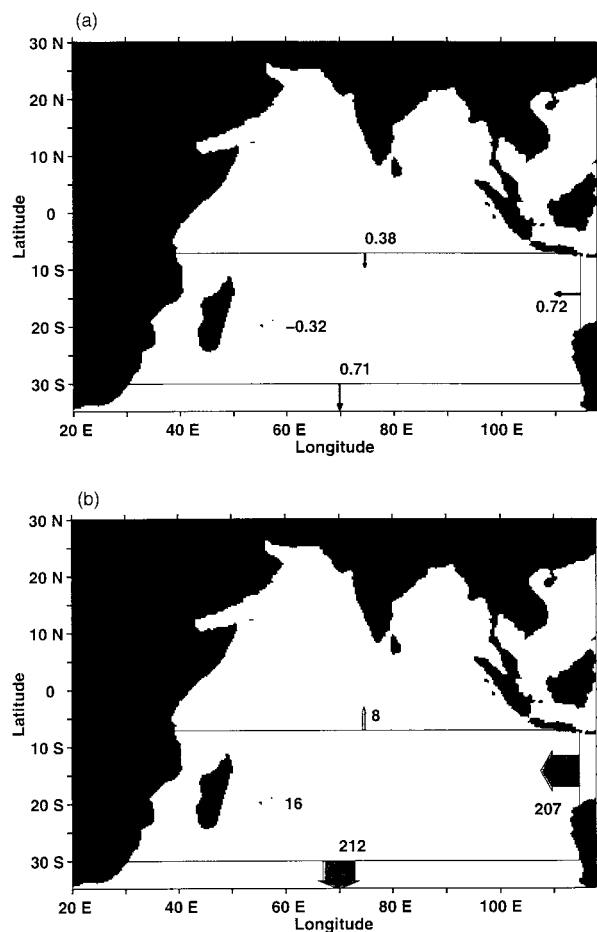
FIG. 8. (a) Temperature fluxes (PW), (b) salt fluxes ($\times 10^6$ kg s^{-1}) in the southern Indian Ocean for 1986–95.

represents the eddy flux. The relative contribution of the eddies to the total flux is about two orders of magnitude smaller than that of the mean term across the 115°E section between Australia and Java for the above cases. Consequently, the transports derived from the mean fields almost entirely represent the total transports through the 115°E section.

Annual net heat transports into the Indian Ocean have been calculated by Hirst and Godfrey (1993) and Schneider and Barnett (1997) using global general circulation models (the latter was coupled to an atmospheric model). They obtained 0.63 and 0.9 PW, respectively, into the Indian Ocean. The net input transport from the POP 10-yr mean field is 0.66 PW, in general agreement with the other models. Differences may be attributed to the model formulations (resolution and friction) and forcing.

To determine the influence of the Indonesian Throughflow waters on the Indian Ocean heat budget, a region encompassing the pathway of the throughflow is examined (Fig. 8a). A closed region is constructed by extracting the total advective heat fluxes along 30°

and 8.5°S, the latter latitude being the northern end of the throughflow section, and between these latitudes along 115°E. Land forms the western boundary of the box, as well as south of 22°S along 115°E. Here the 10-yr mean fields are used. Temperature fluxes are obtained by directly integrating the total advective fluxes along each ocean boundary. Temperature fluxes can be used here as we are interested in the relative contribution of the throughflow waters to the southern Indian Ocean heat budget. The inflow from the Pacific is 0.72 PW, while 0.38 PW enters the region from the northern Indian Ocean across 8.5°S. This net input of 1.1 PW is balanced by 0.71 PW exiting the box at 30°S and 0.32 PW being lost to the atmosphere over the area of the box. The residual is balanced by the change in heat storage over the time of the run (0.08 PW), which represents a loss to the box. Of the heat input to the region, the throughflow represents about 65% of the total. The remaining 35% is from the input of solar radiation to the north of the throughflow. This result is consistent with the recent findings of Garternicht and Schott (1997) who examined the effect of the throughflow on the Indian Ocean heat budget in the Semtner and Chervin ¼° model. The main differences between the models are resolution and the form of the surface heat forcing; in POP, monthly climatological heat fluxes together with a surface temperature restoring term were used, while this version of the Semtner and Chervin model used surface restoring only. In this case, these factors have not significantly changed the effect of the throughflow on the heat budget of the Indian Ocean.

Salt fluxes were obtained directly by integrating $\rho\langle us\rangle$ across the Australia to Java section: for August 1993 and February 1994 they are -251 and -30×10^6 kg s^{-1}, respectively, into the Indian Ocean. The contribution from the mean currents is -246 and -22×10^6 kg s^{-1}, respectively. The eddy contribution is again small.

It should be noted that there is no loss or gain of freshwater in the model; rather salt is added or removed through the effects of the restoring to Levitus (1982) salinities. To understand the impact of the throughflow salt flux on the southern Indian Ocean, salt fluxes are calculated on the boundaries of the box described earlier, again using the 10-yr mean fields (Fig. 8b). Fluxes input to the box are 207×10^6 kg s^{-1} from the throughflow and 16×10^6 kg s^{-1} over the surface of the box. Outputs are 8 and 212×10^6 kg s^{-1} along 8.5°S and 30°S, respectively. The residual is due to subgrid-scale transports since the salt storage term is only -0.1×10^6 kg s^{-1}. Clearly, the throughflow waters dominate the southern Indian Ocean salt budget.

As the model is found to inject too much saline South Pacific thermocline water into the Indian Ocean via the Indonesian seas, it is expected that the model requires less net Indian Ocean evaporation than in reality. The net salt input of 16×10^6 kg s^{-1} requires an equivalent net evaporation of 0.455 Sv consistent with the region

being one of excessive evaporation. Baumgartner and Reichel (1975; Table XXXV, 178) indicates net evaporation of 0.585 Sv for the Indian Ocean between 10° and 30°S. Thus, the equivalent model net evaporation is 78% of the estimated net evaporation.

5. Discussion

Within the Indonesian Seas the Los Alamos Parallel Ocean Program 1/6 deg global model temperature and salinity stratification is dominated by relatively salty South Pacific thermocline water rather than fresher North Pacific thermocline water as found in the Arlindo data. Comparisons of the observations and model fields show that the thermohaline stratification within the Mindanao Current and the New Guinea Coastal Current, the potential sources for the interocean throughflow, match quite closely. This suggests that the thermohaline discrepancies between the model and observed fields within the Indonesian seas stem from regional effects that allow excessive amounts of South Pacific water into the Indonesian seas from north of Irian–Jaya and through Torres Strait, while limiting access of the fresher North Pacific thermocline water through Makassar Strait. It is suspected that the details of the Indonesian seas bottom bathymetry may be the cause for the differences. Examples of inaccurate model bathymetry in key access passages are a 200-m sill in the central Makassar Strait that artificially blocks North Pacific water from freely advecting into the Flores Sea; the artificially deep Torres Strait (50-m model depth vs the less than 10-m observed depth) that allows South Pacific surface water and, perhaps what is more important, the South Pacific subtropical gyre pressure head to pass into the southern Indonesian Seas; and the relatively wide Alor Passage that can accommodate the interocean throughflow without requiring the ''use'' of the deep passage south of Timor, as observed.

A consequence of throughflow transport being dominated by the South Pacific thermocline is that the model North Pacific residence time would be much longer than the real residence time. The $O(10$ Sv$)$ Indonesian Throughflow is the primary exit for the low salinity North Pacific thermocline and intermediate water, as Bering Strait exports only one-tenth of the suspected Indonesian Throughflow magnitude. Reduced export of North Pacific thermocline water implies reduced import via cross equatorial transport of South Pacific water. The model South Pacific water streams directly into the Indian Ocean, without first folding into the North Pacific within the series of zonal equatorial currents. The model North Pacific thermocline is expected therefore to have an unrealistically high degree of isolation from the rest of the World Ocean.

South Pacific–dominated throughflow waters will also impact the salt budget of the southern Indian Ocean, resulting in larger fluxes into the region than are likely to result if the water column was dominated by North

Pacific thermocline water. The heat budget is also likely to be somewhat higher than is realistic as a result of the vertical mixing scheme, which produces too diffuse a thermocline and thus producing warmer temperatures lower in the water column than are observed.

Some of these inadequacies may be remedied by increased vertical and horizontal resolution, and the use of a new global topography dataset obtained from satellite altimetry (Smith and Sandwell 1997). Increasing the number of vertical levels in the upper water column and limiting the depth of the Torres Strait to the top level would reduce the unrealistically high transports through this region. In addition, locally increased friction to mimic the effects of the strong, observed tidal currents would also retard this flow. At deeper locations, an increased number of levels would result in more ''active'' velocity grid points as there is a loss of velocity points adjacent to land. Increased horizontal resolution would better resolve the flow in narrow channels such as Lombok Strait, which currently is only one velocity grid box wide. The Smith and Sandwell (1997) topography dataset, produced by combining shipboard depth soundings with gravity data derived from satellite altimetry, may provide a more realistic bathymetry than that currently used.

Another model inadequacy is the lack of a mixed layer. Presently, the model is unable to distribute momentum to the lower layers, resulting in unrealistically high Ekman flows in the upper level. Inclusion of a mixed layer would remedy this situation and produce a more realistic thermohaline structure in the upper model water column. In addition, a tidal mixing parameterization may produce a more realistic attenuation of water mass properties in the throughflow pathways. Hence, improved bathymetry, increased vertical and horizontal resolution, and the inclusion of a mixed layer and a tidal mixing parameterization will be necessary to more accurately model the Indonesian region.

6. Conclusions

a. Temperature and salinity

Relative to the Arlindo observations, the model thermocline for August 1993 and February 1994 reveals excessive amounts of saline South Pacific water within the Indonesian seas. The model Makassar Strait has a North Pacific–dominated thermocline agreeing with the observational stations to around 250 dbar. Throughflow below that depth is inhibited by a 200-m-deep restriction in the model central Makassar Strait. The model thermohaline stratification within the Maluku, Seram, and Banda Seas is far too salty at all levels except in the surface and deep water, indicating an unrealistically large infusion of South Pacific water. One source of the South Pacific water appears to be through the Halmahera Sea, though the model sill for this region of 500 m is approximately correct. Apparently the model allows ex-

cessive downward mixing of the saline South Pacific water to depths of about 700 dbar (near the 5°C isotherm). The model thermocline appears to be too diffusive, a result of the vertical mixing scheme. The model exports to the Indian Ocean a water column laced with too much South Pacific salt. In the Timor Sea below the 1200-m sill depth that separates the Indonesian seas from the Timor Sea, the model lacks the observed intrusion of saline south Indian Ocean deep water.

b. Mass, heat and salt fluxes

The pathways of the interocean throughflow within the model do not agree with the observationally derived inference, though the observational base is weak. Within the model, North Pacific thermocline water flowing through the upper 200 m of the Makassar Strait exits the Indonesian seas in the Lombok Strait (the same is found in the Miyama et al. 1995 model results), whereas the observations show that the bulk turns eastward into the Flores and Banda Seas before exiting the Indonesian seas near Timor. A major discrepancy in the surface layer velocity field between the model and observations, with possible overall transport ramifications, arises from the wide, 50-m-deep model Torres Strait, through which the model permits an unrealistically large seasonal exchange between the Coral Sea and the Indonesian seas. Closing the Torres Strait within the model would be expected not only to block the water mass exchange but also alter the transmission of the South Pacific pressure head from the axis of the South Pacific subtropical gyre within the Coral Sea. This closing could have the far reaching effect of increasing the access within the model of the tropical Pacific water into the northern Indonesian seas, leading to a more realistic throughflow configuration.

The model Pacific to Indian throughflow transport values (7 Sv for August 1993 and 0.6 Sv for February 1994) are slightly lower than expected in comparison with the limited set of observations. The Meyers (1996) XBT study indicates lower than normal throughflow transports for October 1993 to April 1994. This is believed to be a response to the weak El Niño condition during that time. The 1988 and 1989 (La Niña phase) model results do show increased transports closer to the observed values. A better view of simulated interannual variability could also be obtained by using consistent 10-m wind forcing throughout the period 1979–1995, which will become possible through an ongoing ECMWF reanalysis project using their best contemporary model.

The throughflow exports 0.66 PW of heat from the Pacific to the Indian Oceans. This estimate is in general agreement with values obtained from other general circulation models (Hirst and Godfrey 1993; Schneider and Barnett 1997). The throughflow waters contribute about 65% of the total heat input to the southern Indian Ocean while the other 35% comes from the accumulation of

solar radiation north of the throughflow. In addition, the throughflow salt flux dominates the input to this region. The model throughflow of excessive amounts of South Pacific thermocline water requires smaller model net evaporation in the subtropical Indian Ocean than expected from observational-based estimates.

REFERENCES

Barnier, B., L. Siefridt, and P. Marchesiello, 1995: Thermal forcing for a global ocean circulation model using a three-year climatology of ECMWF analyses. *J. Mar. Syst.,* **6,** 363–380.

Baumgartner, A., and E. Reichel, 1975: *The World Water Balance.* Elsevier, 179 pp.

Bingham, F., and R. Lukas, 1994: The southward intrusion of North Pacific Water along the Mindanao Current. *J. Phys. Oceanogr.,* **24,** 141–154.

Broecker, W. S., W. C. Patzert, R. Toggweiler, and M. Stuiver, 1986: Chemistry and radioisotopes in the southeast Asian basins. *J. Geophys. Res.,* **91** (C12), 14 345–14 354.

Bryan, F., 1987: Parameter sensitivity of primitive equation ocean general circulation models. *J. Phys. Oceanogr.,* **17,** 970–985.

Bryan, K., 1969: A numerical method for the study of the world ocean. *J. Comput. Phys.,* **4,** 347–376.

Cox, M. D., 1970: A mathematical model of the Indian Ocean. *Deep-Sea Res.,* **17,** 45–75.

——, 1984: A primitive equation three-dimensional model of the ocean. GFDL Ocean Group Tech. Rep. No. 1, Geophysical Fluid Dynamics Laboratory/NOAA.

Cresswell, G., A. Frische, J. Peterson, and D. Quadfasel, 1993: Circulation in the Timor Sea. *J. Geophys. Res.,* **98** (C8), 14 379–14 390.

Ffield, A., and A. L. Gordon, 1992: Vertical mixing in the Indonesian Thermocline. *J. Phys. Oceanogr.,* **22,** 184–195.

——, and ——, 1996: Tidal mixing signatures in the Indonesian Seas. *J. Phys. Oceanogr.,* **26,** 1924–1937.

Fieux, M., C. Andrié, P. Delecluse, A. G. Ilahude, A. Kartavtseff, F. Mantisi, R. Molcard, and J. C. Swallow, 1994: Measurements within the Pacific–Indian Ocean throughflow region. *Deep-Sea Res.,* **41,** 1091–1130.

——, R. Molcard, and A. G. Ilahude, 1996: Geostrophic transport of the Pacific–Indian Oceans throughflow. *J. Geophys. Res.,* **101** (C5), 12 421–12 432.

Fine, R. A., 1985: Direct evidence using tritium data for throughflow from the Pacific into the Indian Ocean. *Nature,* **315,** 478–480.

Fine, R., R. Lukas, F. Bingham, M. Warner, and R. Gammon, 1994: The western equatorial Pacific: A water mass crossroads. *J. Geophys. Res.,* **99** (C12), 25 063–25 080.

Fu, L.-L., 1986: Mass, heat and freshwater fluxes in the South Indian Ocean. *J. Phys. Oceanogr.,* **16,** 1683–1693.

——, and R. D. Smith, 1996: Global ocean circulation from satellite altimetry and high-resolution computer simulation. *Bull. Amer. Meteor. Soc.,* **77,** 2625–2636.

Garternicht, U., and F. Schott, 1997: Heat fluxes of the Indian Ocean from a global eddy-resolving model. *J. Geophys. Res.,* **102,** 21 147–21 159.

Godfrey, J. S., 1996: The effect of the Indonesian throughflow on ocean circulation and heat exchange with the atmosphere: A review. *J. Geophys Res.,* **101** (C5), 12 217–12 237.

——, and T. J. Golding, 1981: Sverdrup relation in the Indian Ocean, and the effect of Pacific–Indian Ocean throughflow on Indian Ocean circulation and on the East Australian Current. *J. Phys. Oceanogr.,* **11,** 771–779.

Gordon, A. L., 1986: Interocean exchange of thermocline water. *J. Geophys. Res.,* **91** (C4), 5037–5047.

——, 1995: When is ''appearance'' reality? Indonesian Throughflow is primarily derived from North Pacific water masses. *J. Phys. Oceangr.,* **25,** 1560–1567.

——, and R. Fine, 1996: Pathways of water between the Pacific and Indian Oceans in the Indonesian seas. *Nature,* **379** (6561), 146–149.

——, A. Ffield, and A. G. Ilahude, 1994: Thermocline of the Flores and Banda Seas. *J. Geophys. Res.,* **99** (C9), 18 235–18 242.

Hall, M. M., and H. L. Bryden, 1982: Direct estimates and mechanisms of ocean heat transport. *Deep-Sea Res.,* **29,** 339–359.

Hautala, S., J. Reid, and N. Bray, 1996: The distribution and mixing of Pacific water masses in the Indonesian seas. *J. Geophys. Res.,* **101** (C5), 12 375–12 389.

Hirst, A. C., and J. S. Godfrey, 1993: The role of Indonesian Throughflow in a global ocean GCM. *J. Phys. Oceanogr.,* **23,** 1057–1086.

Ilahude, A. G., and A. L. Gordon, 1996: Thermocline stratification within the Indonesian Seas. *J. Geophys. Res.,* **101** (C5), 12 401–12 409.

Kindle, J. C., H. E. Hurlburt, and E. J. Metzger, 1989: On the seasonal and interannual variability of the Pacific to Indian Ocean throughflow. *Proc. Western Pacific Int. Meeting and Workshop on TOGA COARE,* Noumea, New Caledonia, 355–365. [Available from Centre ORSTOM de Noumea, B.P. A5 98848, Noumea Cedex, New Caledonia.]

Levitus, S., 1982: *Climatological Atlas of the World Ocean.* NOAA Prof. Paper No. 13, U.S. Govt. Printing Office, 173 pp.

MacDonald, A., 1993: Property fluxes at 30°S and their implications for the Pacific–Indian Throughflow and the global heat budget. *J. Geophys. Res.,* **98** (C4), 6851–6868.

Maltrud, M. E., R. D. Smith, A. J. Semtner, and R. C. Malone, 1998: Global eddy-resolving ocean simulations driven by 1985–1994 atmospheric winds. *J. Geophys. Res.,* in press.

McClean, J. L, A. J. Semtner, and V. Zlotnicki, 1997: Comparisons of mesoscale variability in the Semtner–Chervin quarter-degree model, the Los Alamos POP sixth-degree model, and the TO-PEX/POSEIDON data. *J. Geophys. Res.,* **102** (C11), 25 203–25 226.

Meyers, G. 1996: Variations of Indonesian Throughflow and ENSO. *J. Geophys. Res.,* **101** (C5), 12 255–12 263.

——, R. Bailey, and A. Worby, 1995: Volume transport of Indonesian throughflow. *Deep-Sea Res.,* **42** (7), 1163–1174.

Miyama, T., T. Awaji, K. Akitomo, and N. Imasato, 1995: Study of seasonal transport variations in the Indonesian seas. *J. Geophys. Res.,* **100** (C10), 20 517–20 541.

Molcard, R., M. Fieux, J. Swallow, A. Ilahude, and J. Banjarnahor, 1994: Low frequency variations of currents in the Indonesian channels. *Deep-Sea Res.,* **41** (Part I), 1643–1661.

——, ——, and A. Ilahude, 1996: The Indo–Pacific throughflow in the Timor Passage. *J. Geophys. Res.,* **101** (C5), 12 411–12 420.

Murray, S. P., and D. Arief, 1988: Throughflow into the Indian Ocean through the Lombok Strait. January 1985–January 1986. *Nature,* **333,** 444–447.

——, ——, J. C. Kindle, and H. E. Hurlburt, 1989: Characteristics of circulation in an Indonesian Archipelago Strait from hydrography, current measurements and modeling results. *NATO Advanced Research Workshop on The Physical Oceanography of Sea Straits,* Les Arcs, France, Kluwer Academic.

Pacanowski, R., and S.G.H. Philander, 1981: Parameterization of vertical mixing in numerical models of tropical oceans. *J. Phys. Oceanogr.,* **11,** 176–189.

Piola, A. R। and A. Gordon, 1984: Pacific and Indian Ocean upper layer salinity budget. *J. Phys. Oceanogr.,* **14,** 747–753.

Schneider, N., and T. Barnett, 1997: Indonesian throughflow in a coupled general circulation model. *J. Geophys. Res.,* **102,** 12 341–12 358.

Schott, F. A., and C. W. Böning, 1991: The WOCE model in the western equatorial Atlantic: upper layer circulation. *J. Geophys. Res.,* **96,** 6993–7004.

Semtner, A. J., 1974: An oceanic general circulation model with bottom topography. Tech. Rep. 9, Dept. of Meteorology, University of California, Los Angeles, 99 pp. [Available from A. Gordon, Lamont-Doherty Earth Observatory, Columbia University, Palisades, NY 10964-8000.]

——, 1997: Very high-resolution estimates of global ocean circulation, suitable for carbon-cycle modeling. *Proc. 1993 Snowmass Global Change Institute on the Global Carbon Cycle,* T. Wigley, Ed. Cambridge University Press, in press.

——, and R. M. Chervin, 1988: A simulation of the global ocean circulation with resolved eddies. *J. Geophys. Res.,* **93,** 15 502–15 522 and 15 767–15 775.

——, and ——, 1992: Ocean general circulation from a global eddy-resolving model. *J. Geophys. Res.,* **97,** 5493–5550.

Smith, R. D., J. K. Dukowicz, and R. C. Malone, 1992: Parallel ocean general circulation modeling. *Physica D,* **60,** 38–61.

Smith, W. F., and D. T. Sandwell, 1997: Global seafloor topography from satellite altimetry and ship depth soundings. *Science,* **277,** 1956–1962.

Talley, L. D., 1984: Meridional heat transport in the Pacific Ocean. *J. Phys. Oceanogr.,* **14,** 231–241.

Tourre, Y. M., and W. B. White, 1995: ENSO signals in global upper-ocean temperature. *J. Phys. Oceanogr.,* **25,** 1317–1332.

van Aken, H. M., J. Punjanan, and S. Saimima, 1988: Physical aspects of the flushing of the East Indonesian basins. *Neth. J. Sea Res.,* **22,** 315–339.

Van Bennekom, A., 1988: Deep-water transit times in the eastern Indonesian basins, calculated from dissolved silica in deep and interstitial waters. *Neth. J. Sea Res.,* **22** (4), 341–354.

Wolanski, E., P. Ridd, and M. Inoue, 1988: Currents through Torres Strait. *J. Phys Oceanogr.,* **18,** 1535–1545.

Wyrtki, K., 1961: Scientific results of marine investigations of the South China Sea and the Gulf of Thailand. Physical oceanography of the Southeast Asian waters, NAGA Rep. 2, Scripps Inst. Oceanography, University of California, San Diego, 195 pp. [Available from Scripps Institution of Oceanography, University of California, San Diego, La Jolla, CA 92093.]

——, 1987: Indonesian throughflow and the associated pressure gradient. *J. Geophys. Res.,* **92,** 12 941–12 946.

——, 1989: Some thoughts about the West Pacific Warm Pool. *Proc. Western Pacific Int. Meeting and Workshop on TOGA/COARE,* Noumea, New Caledonia, 99–109. [Available from Centre OR-STOM de Noumea, B.P. A5 98848, Noumea Cedex, New Caledonia.]